Unusual large magnetostriction in the ferrimagnet $Gd_{2/3}Ca_{1/3}MnO_3$

To cite this article: V. F. Correa *et al* 2012 *EPL* **98** 37003

A Letters Journal Exploring the Frontiers of Physics

May 2012

EPL, **98** (2012) 37003
doi: 10.1209/0295-5075/98/37003

www.epljournal.org

Unusual large magnetostriction in the ferrimagnet $Gd_{2/3}Ca_{1/3}MnO_3$

V. F. Correa[(a)], N. Haberkorn, G. Nieva, D. J. García and B. Alascio

Centro Atómico Bariloche (CNEA) and Instituto Balseiro (U. N. Cuyo) - 8400 Bariloche, Río Negro, Argentina

received 2 March 2012; accepted in final form 12 April 2012
published online 11 May 2012

PACS 75.80.+q – Magnetomechanical effects, magnetostriction
PACS 75.50.Gg – Ferrimagnetics
PACS 75.47.Lx – Magnetic oxides

Abstract – We report an unusual large linear magnetostrictive effect in the ferrimagnet $Gd_{2/3}Ca_{1/3}MnO_3$ ($T_c \approx 80\,K$). Remarkably, the magnetostriction, negative at high temperature ($T \approx T_c$), becomes positive below 15 K when the magnetization of the Gd sublattice overcomes the magnetization of the Mn sublattice. A rather simple model where the magnetic energy competes against the elastic energy gives a good account of the observed results and confirms that Gd plays a crucial role in this unusual observation. Unlike previous works in manganites where only striction associated with $3d$ Mn orbitals is considered, our results show that the lanthanide $4f$-orbitals–related striction can be very important too and it cannot be disregarded.

Introduction. – Manganites are perovskites mostly known for their spectacular colossal magnetoresistance (CMR): the electrical resistivity can change by several orders of magnitude under a moderate applied magnetic field B [1]. They also show another impressive property: a large linear magnetostriction (MS) where the sample dimensions are strongly affected by a magnetic field, either external or molecular [2]. The effect is comparable in magnitude ($\Delta L/L \geqslant 10^{-3}$ at several teslas) to the highest MS values ever reported. Both CMR and MS are particularly large around the Mn-ions ferromagnetic ordering temperature [3]. Associated with this order, and depending on the doping level, manganites can display a metal-insulator (MI) transition, too. In this way, manganites offer a unique testing ground to study the interplay between electronic, spin and lattice degrees of freedom.

As expected, the structural distortion of the plain perovskite structure strongly affects the magnetic and electronic properties of the manganites. This is usually parametrized by the so-called tolerance factor t, which quantifies the mismatch between the different ion sizes in the formula. This mismatch primarily influences the exchange interaction between Mn ions altering both the length and the angle of the Mn-O-Mn bond. A "*universal*" temperature T *vs.* $t = (d_{R/A\text{-}O})/\sqrt{2}(d_{Mn\text{-}O})$ phase diagram has long been reported [4] for the hole doped $R_{2/3}A_{1/3}MnO_3$ manganites (R being a lanthanide and A being an alkaline-earth element). Slightly distorted structures ($t \sim 1$) show an insulating-paramagnet (PMI) to metallic-ferromagnet (FMM) transition. However, the metallic state disappears at higher distortions ($t \lesssim 0.91$) even though a transition to an insulating-ferromagnet (FMI) is observed.

An estimated value of $t \approx 0.89$ places $Gd_{2/3}Ca_{1/3}MnO_3$ well inside the insulating regime. Indeed, no MI transition is observed down to 5 K with the resistivity ρ showing a characteristic semiconducting behavior in the whole temperature range [5,6]. Nevertheless, the magnetic properties are quite unusual. Mn magnetic moments start ordering ferromagnetically around $T_c \sim 80\,K$. The Gd moments react to the internal field created by the Mn ferromagnetic sublattice gradually aligning in the opposite direction. The two sublattices compete with each other giving rise first to a maximum in the magnetization around 50 K and finally to a full compensation at $T_{comp} \sim 15\,K$ where the magnetization vanishes. At lower temperature, the Gd magnetic moment overcomes the Mn moment. The overall temperature dependence of the magnetization corresponds then to a ferrimagnet created by the two opposite Mn and Gd sublattices [5,7–9].

In this work we study the magnetostructural properties of $Gd_{2/3}Ca_{1/3}MnO_3$. The rather complex magnetic structure clearly couples to the atomic lattice giving rise to a large linear magnetostrictive effect [10]. Remarkably,

[(a)] E-mail: victor.correa@cab.cnea.gov.ar

the negative field dependence of the MS observed at high temperature changes its sign and becomes positive when $T < T_{comp}$. We use a 4-site mean-field approximation to model the experimental data. The model demonstrates that the competition between Gd-Gd and Gd-Mn spin correlations is responsible for the sign change in the MS. This finding shows that the usually underestimated MS associated with the lanthanide $4f$ orbitals in manganites can be comparable to the usual large striction given by the re-orientation of the Mn $3d$ orbitals.

Experimental details. – Pure single crystals of $Gd_{2/3}Ca_{1/3}MnO_3$ were grown by the floating-zone technique. Crystal quality and composition have been checked through XRD and EDS scans. A capacitive technique was used in the dilation experiments. The high resolution ($\leqslant 1$ Å) dilatometer [11] is placed in an evacuated environment with a low pressure ($P < 10^{-1}$ torr) of exchange ^{4}He gas. The magnetic field is applied along the [020] direction of the orthorhombic *Pnma* crystalline structure ($a = 5.39$ Å, $b = 5.56$ Å and $c = 7.5$ Å) in all the experiments. Sample length L is typically about 200 μm. Dilation experiments are always performed in a longitudinal configuration with $B \parallel L \parallel$ [020]. Several samples of different size have been measured with a perfect agreement between them.

Results and discussion. – Representative isothermal linear magnetostriction results, after a zero-field-cooling procedure, are shown in fig. 1 (solid lines). The effect is very large with no evidence of saturation up to $B = 12$ T (the highest applied field), reaching a maximum value around $T_c \sim 80$ K ($\Delta L/L \approx 10^{-3}$). Two very distinctive regimes are found:

i) above $T_{comp} \sim 15$ K the field dependence of L is negative and monotonic. Hysteresis and relaxation effects are important, mainly in the range $40\,\mathrm{K} \lesssim T \lesssim T_c$,

ii) below T_{comp} magnetostriction becomes positive at low fields $B \leqslant 7$ T (the initial negative slope at $B < 1$ T is associated to magnetic domains and is absent if the experiment is performed after a field cooling procedure). At higher fields it turns negative again resulting in an overall non-monotonic field dependence of the MS. On the other hand, around T_{comp} (where the magnetization almost vanishes), the magnetostriction is negligible below $B \sim 4$ T.

T_{comp} marks the onset of the Gd magnetic ordering which dominates the low temperature regime while Mn moments prevail in the high-temperature regime. In this sense, this unusual magnetostriction strongly points toward the interplay of the different magnetic interactions: Mn-Mn, Mn-Gd and Gd-Gd. We use a simple model to verify this hypothesis where the three different interactions are introduced in the Hamiltonian via Heisenberg-like terms.

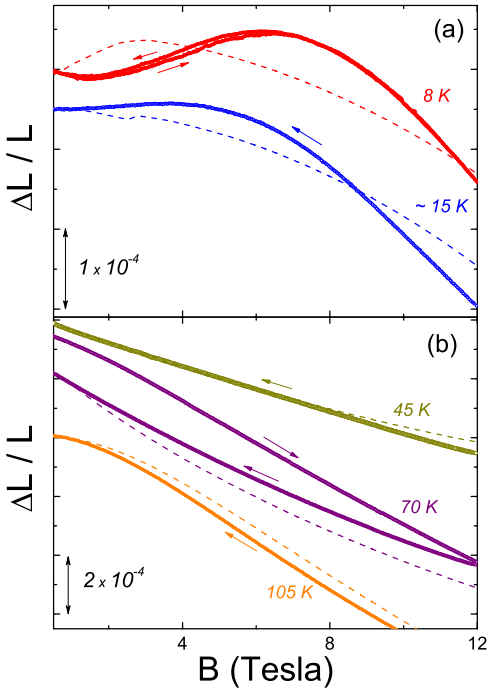

Fig. 1: (Color online) Experimental (solid) and calculated (dashed) magnetostriction. The upper (lower) panel shows results in the low (high) temperature range. Arrows stand for the direction of the field sweep. Curves are vertically shifted.

We consider a homogeneous network of Gd ions with one Gd ion for each Mn, ignoring the random nature of their localizations. Also, as there are 2/3 Gd ions for each Mn, we rescale the Gd effective magnetic moment to $J = 2/3 \times 7/2 = 7/3 \sim 5/2$. We choose the 5/2 value for the Gd spin to retain the quantum nature of the spin without rescaling of the g-factor ($g_{Gd} = 2$). Manganese ions appear in a mixture of 1/3 with $S = 3/2$ and 2/3 with $S = 2$. As in both cases the orbital magnetic moment is quenched, we take $g_{Mn} = 2$. To keep the experimental zero temperature net magnetic moment of $1\,\mu_B$ (perfect ferrimagnetic ordering given by the two sublattices [5]) we take $S = 2$ for the Mn effective magnetic moment.

Based on these considerations we write a Hamiltonian with a ferromagnetic (coupling $K_{Mn\text{-}Mn}$) network of manganese spins S ($S = 2$) antiferromagnetically coupled ($K_{Mn\text{-}Gd}$) to a network of ferromagnetic ($K_{Gd\text{-}Gd}$) gadolinium spins J ($J = 5/2$). The magnetic interaction is given by the Hamiltonian

$$H_m = K_{Mn\text{-}Mn} \sum_{\langle i,j \rangle} S_i \cdot S_j + K_{Mn\text{-}Gd} \sum_i S_i \cdot J_i + K_{Gd\text{-}Gd} \sum_{\langle i,j \rangle} J_i \cdot J_j + g\mu_B \vec{B} \cdot \sum_i (S_i + J_i). \quad (1)$$

The smaller values of the effective spins allow us to use a 4-site (2 Mn and 2 Gd) cluster in the constant coupling approximation (see appendix) [12–14]. We consider six nearest neighbours ($z = 6$). In the constant coupling

approximation the interactions are isotropic, meaning that they represent averaged interactions.

Following early works [14–16], we consider that the exchange parameters are strain dependent. If the lattice is under some small distortion δ_L, all the coupling parameters change accordingly:

$$\begin{aligned} K_{Mn\text{-}Mn} &= K^0_{Mn\text{-}Mn} + \alpha\delta_L, \\ K_{Mn\text{-}Gd} &= K^0_{Mn\text{-}Gd} + \beta\delta_L, \\ K_{Gd\text{-}Gd} &= K^0_{Gd\text{-}Gd} + \gamma\delta_L. \end{aligned} \tag{2}$$

From fits to magnetization experiments, we obtain: $K^0_{Mn\text{-}Mn} = -9\,\mathrm{K}$, $K^0_{Mn\text{-}Gd} = 8\,\mathrm{K}$ and $K^0_{Gd\text{-}Gd} = 0\,\mathrm{K}$. Mn-Mn coupling $K^0_{Mn\text{-}Mn}$ is ferromagnetic with T_c close to the experimental value of ∼80 K; $K^0_{Mn\text{-}Gd}$ is antiferromagnetic and gives $T_{comp} \sim 15\,\mathrm{K}$ together with an effective null coupling between Gd ions (also expected due to the dipolar origin of those interactions). Both, our experimental and calculated magnetization results are similar to those reported by Snyder *et al.* [5].

The presence of a distortion also increases the elastic energy

$$E_e = 1/2C\delta_L^2, \tag{3}$$

where C is the elastic constant.

For a state $|G\rangle$, the total energy $E_m + E_e$ is minimized for

$$\begin{aligned} \delta_L(B) = -\frac{1}{C}\langle G|\alpha\sum S_i\cdot S_j + \beta\sum S_i\cdot J_i \\ +\gamma\sum J_i\cdot J_j|G\rangle_B. \end{aligned}$$

As we are interested in the length distortion with respect to the $B = 0$ case, we compute

$$\begin{aligned} \frac{\Delta L}{L} &= \delta_L(B) - \delta_L(0) \\ &= \Lambda_\alpha(\langle G|\sum_{\langle i,j\rangle} S_i\cdot S_j|G\rangle_{B=0} - \langle G|\sum_{\langle i,j\rangle} S_i\cdot S_j|G\rangle_B) \\ &+ \Lambda_\beta(\langle G|\sum_{i} S_i\cdot J_i|G\rangle_{B=0} - \langle G|\sum_{i} S_i\cdot J_i|G\rangle_B) \\ &+ \Lambda_\gamma(\langle G|\sum_{\langle i,j\rangle} J_i\cdot J_j|G\rangle_{B=0} - \langle G|\sum_{\langle i,j\rangle} J_i\cdot S_j|G\rangle_B), \end{aligned} \tag{4}$$

where $\Lambda_\chi = \frac{\chi}{C}$ and $\chi = \{\alpha, \beta, \gamma\}$. $\langle\rangle_B$ denotes the thermal expectation value.

The correlations are computed using the 4-site Constant Coupling approximation and correspondingly now $i, j = 1, 2$. Figure 2 shows the computed spin correlators as a function of magnetic field ($\Delta\langle O\rangle = \langle O\rangle_B - \langle O\rangle_{B=0}$, where $O = S_1\cdot S_2, S_1\cdot J_1$ or $J_1\cdot J_2$) in the different temperature ranges: below, around and above T_{comp}.

There are several issues to emphasize:

i) the field dependence of the Mn-Mn correlations ($\Delta\langle S_1\cdot S_2\rangle$) is monotonic and, except around T_c, it is also very small (fig. 2(a)), reflecting the fact that Mn sublattice is almost fully polarized at low temperature.

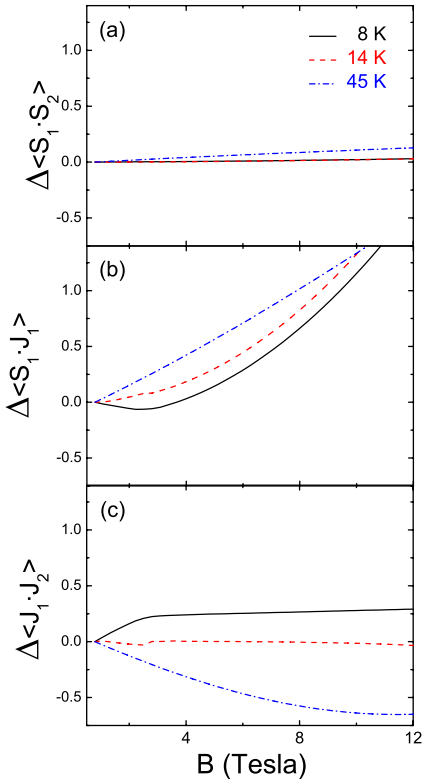

Fig. 2: (Color online) Computed correlations change with respect to the zero-field situation for 8 K (below T_{comp}), 14 K (close to T_{comp}) and 45 K (above T_{comp}). (a) Mn-Mn correlations, (b)Mn-Gd correlations and (c) Gd-Gd correlations.

ii) Mn-Gd correlations ($\Delta\langle S_1\cdot J_1\rangle$) show the largest effect below T_c, as seen in fig. 2(b). This is reasonable since the applied field tends to align both sublattices in the same direction gradually destroying the otherwise almost perfect low temperature ferrimagnet. Its contribution to the low-field total magnetostriction, however, is smaller than that due to Gd-Gd correlations by a factor $\frac{1}{4}$ approximately. At higher fields, on the other hand, $\Delta\langle S_1\cdot J_2\rangle$ becomes the larger contribution.

iii) Gd-Gd correlations ($\Delta\langle J_1\cdot J_2\rangle$) show the most relevant and distinct behavior. While $\Delta\langle J_1\cdot J_2\rangle$ is negative for $T > T_{comp}$, it vanishes around T_{comp} and becomes positive when $T < T_{comp}$. The physical origin of this sign change is related to the local field acting on the Gd moments. This local field is made up of the molecular field created by the Mn moment B_{Mn} plus the external field B. Above T_{comp}, B_{Mn} points opposite to B so an increasing B ($B < B_{Mn}$) results in a decreasing local field. This decreasing local field reduces the Gd moment and consequently the Gd-Gd correlations. Below T_{comp}, on the other hand, B_{Mn}

points in the same direction of B, so an increasing B ($B < B_{Mn}$) results in a increasing local field. This increasing local field rises the Gd-Gd correlations. This sign inversion in the Gd-Gd correlations is indeed responsible for the observed sign change in the magnetostriction at low temperature.

Computed MS curves are also shown in fig. 1 ($\Lambda_\alpha = 12 \times 10^{-4}$, $\Lambda_\beta = 0.8 \times 10^{-4}$ and $\Lambda_\gamma = -1.6 \times 10^{-4}$). We choose Λ_α to get a good agreement at high temperature ($T \geqslant T_c$) where the only non-negligible correlator is $\Delta\langle S_1 \cdot S_2\rangle$ while Λ_γ is chosen as to get a positive striction at low temperature and field ($T < T_{comp}$, $B \leqslant 5\,\mathrm{T}$) where only $\Delta\langle J_1 \cdot J_2\rangle$ is non-negligible. Λ_β is then selected to get the best agreement (with the decreasing field curves) in the whole temperature and field range.

The model gives a good account for the non-monotonic $\Delta L/L$ below T_{comp} (see curve at 8 K, fig. 1(a)). It is a consequence of two opposite contributions: a negative Gd-Gd magnetostructural coupling ($\Lambda_\gamma < 0$) and a positive Mn-Gd coupling ($\Lambda_\beta > 0$). As stated previously, Mn-Mn correlations are almost saturated and they do not contribute to the MS in this low-temperature range. The coupling parameters (K's) used (fixed by the fit of the magnetic properties) allow us to reproduce qualitatively the field value of the MS maximum. The model also accounts for the extinction of this maximum at $T_{comp} \sim 15\,\mathrm{K}$, where the striction becomes very small.

At higher T ($T_{comp} \leqslant T \ll T_c$) the MS gets negative. As before, Mn-Mn correlations almost do not change, but now both Gd-Mn and Gd-Gd correlation effects point in the same direction. In the intermediate- and high-temperature range ($T \gg T_{comp}$), where the Mn-Mn contribution is the most relevant one, the agreement is fairly good, except around T_c. Not only the magnitude of the magnetostriction is well accounted for, also the curvature of the isotherms is very well reproduced (see fig. 1(b)). It is interesting to stress that even though the magnetization is an increasing function of the field in the whole temperature range, the magnetic correlations, and so magnetostriction, show two very distinctive regimes: a monotonic magnetostriction at high temperature that becomes non-monotonic below T_{comp}.

In this isotropic model, C can be estimated as vB_T, where v is the volume of the perovskite unit cell and B_T is the bulk modulus. The Mn-Mn parameter Λ_α is positive, and so is α. Since the interaction is FM ($K_{Mn\text{-}Mn} < 0$), this implies that $|K_{Mn\text{-}Mn}|$ increases as the lattice gets smaller. This is the expected behavior for exchange-like interactions. There are no available pressure effects on $Gd_{2/3}Ca_{1/3}MnO_3$ to compare with. Nevertheless, a rough estimate can be done by replacing Gd by another lanthanide, *i.e.* by chemical pressure. This substitution (keeping the composition at $R_{2/3}Ca_{1/3}MnO_3$) does not modify the Mn valence and so, its magnetic moment. So, a change in T_c can in principle be associated with an inter-ion distance d change. In this isotropic approximation, $d = v^{1/3}$. Taking $B_T = 150\,\mathrm{Gpa}$ [17], and $v = 55.36\,\text{Å}^3$, [7] we get $\alpha = 722\,\mathrm{K}$. For $Dy_{2/3}Ca_{1/3}MnO_3$, $v_{Dy} \approx 55.10\,\text{Å}^3$ [18]. This results in a change of the exchange parameter $K_{Mn\text{-}Mn}$ given by $\Delta K = \alpha \frac{d_{Dy} - d_{Gd}}{d_{Dy}} \approx -2\,\mathrm{K}$. This very rough estimate of a 20 percent increase in the exchange parameter ($K_{Mn\text{-}Mn} = -9\,\mathrm{K}$) is of the same order of magnitude that the T_c increase observed in $Dy_{2/3}Ca_{1/3}MnO_3$ [19].

Gd-Gd parameter Λ_γ is negative and it may be related to the dipolar (anisotropic) origin of these interactions: for zero distortion the net (average) interaction is zero but when the lattice shrinks AF interactions prevail. Notably, the magnetostriction associated with Gd (low field positive striction below T_{comp}) is of the same order of magnitude than the observed striction in metallic gadolinium [14]. On the other hand, the Mn-Gd parameter Λ_β is positive and it is much more difficult to understand since Mn-Gd interactions are antiferromagnetic: this effective interaction diminishes as the lattice shrinks. This counterintuitive value of Λ_β could be related with the rotation of the oxygen tetrahedra that surrounds Mn ions.

Conclusions. – An unusual non-monotonic large magnetostriction is observed in single crystals of the ferrimagnet $Gd_{2/3}Ca_{1/3}MnO_3$ at low temperature ($T < T_{comp} \sim 15\,\mathrm{K}$) arising from the interplay between the Mn and Gd magnetic sublattices. A simple mean-field approximation where different magnetic interactions (Gd-Gd, Mn-Mn and Mn-Gd) compete among them and with the elastic energy gives a good account of the observed results. Particularly, the change in the sign of the magnetostrictive effect at low temperature is driven by the competition between Mn-Gd and Gd-Gd magnetic correlations and it does not involve the Mn-Mn correlations. Unlike previous works [20] in manganites, where only striction associated with d orbitals is considered, our results show that f-orbitals–related striction can be important, too.

* * *

We thank M. T. Causa, L. Manuel, C. Balseiro and A. Aligia for fruitful discussions. The authors are members of CONICET, Argentina. Work partially supported by ANPCyT PICT05-32900, PICT07-00812, PICT07-00819, PICT08-1043 and SeCTyP-UNCuyo 06/C326.

Appendix: constant coupling approximation. – The constant coupling (CC) approximation [12–14] is an improvement over a classical mean-field approximation. It allows to consider correlations and to obtain a critical temperature closer to the exact result. A classical mean-field approximation replaces all the interactions of a site by an effective magnetic field made up of the external

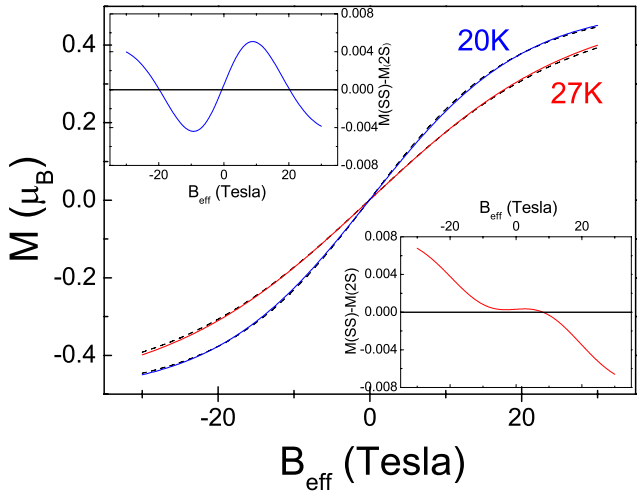

Fig. 3: (Color online) Main panel: magnetization as a function of the effective field for a single site (black dotted lines) and a two-site cluster (solid colored lines) taking $S = 1/2$, $K = 30\,\mathrm{K}$ and $z = 6$. The upper (lower) inset shows the magnetization difference at 20 K (27 K). The classical mean-field transition temperature is $T_{C,MF} = 2/3zS(S+1)K = 90\,\mathrm{K}$.

field and its neighbours magnetization. This neighbours magnetization is assumed to be the same as that of the site. In the constant coupling approximation two systems must give identical results for the magnetization. If the original problem is in a network with z neighbours per site, one system is made with a single site and z "effective" neighbours, while the other is made up with a cluster of 2 sites and $z-1$ "effective" neighbours for each site. In a classical mean field we have to search for an effective field proportional to the neighbours magnetization. The CC approximation consists in searching for an effective field in both systems such that the same magnetization is obtained in the single site and the cluster.

To illustrate the procedure we use a simple spin-(1/2) ferromagnet. For a single site the Hamiltonian is written as

$$H_{ss} = g\mu_B(z\vec{B}_{eff} + \vec{B}) \cdot S,$$

where B_{eff} is an effective field. In a classical mean-field approximation $B_{eff} = K_{Mn\text{-}Mn}\langle S\rangle$ and a self-consistent $\langle S\rangle$ is looked for. For a two-site cluster the Hamiltonian is

$$H_{2s} = KS_1 \cdot S_2 + g\mu_B \left[(z-1)\vec{B}_{eff} + \vec{B}\right] \cdot [S_1 + S_2]\,.$$

In fig. 3 we show the magnetization at high temperature (27 K, just above the transition) of both a single site and a cluster of two sites as a function of B_{eff} with an applied external field $B = 0.1\,\mathrm{T}$. These magnetizations are zero for $(z-1)B_{eff} = -B$ (or $zB_{eff} = -B$ for a single site) and show the expected paramagnetic-like behaviour for small systems. At temperatures above the transition temperature both magnetizations agree for a single field (lower inset) which is then, the right effective field (around 7 T for this temperature; the corresponding magnetization is less than $0.1\,\mu_B$). As the temperature lowers, this solution moves toward higher fields with a corresponding larger magnetization. Below the transition temperature, two new solutions (higher in energy) appear, just as in a regular mean-field approximation (upper inset).

For the ferrimagnet $Gd_{2/3}Ca_{1/3}MnO_3$ we take as the "single" site a unit made up of an effective manganese ($S = 2$, $g = 2$) and an effective Gd ($J = 5/2$, $g = 2$) ion

$$\begin{aligned} H_{ss} \;=\; & g\mu_B(z\vec{B}_{eff,Mn} + \vec{B}) \cdot S \\ & + g\mu_B(z\vec{B}_{eff,Gd} + \vec{B}) \cdot J \\ & + K_{Gd\text{-}Mn} S \cdot J. \end{aligned}$$

The cluster is made with two Mn and two Gd ions and we take $z = 6$. Each Mn (Gd) ion interacts with the other and with an external field made by the $z-1$ remaining neighbours. In each site, there is a Gd-Mn interaction. The Hamiltonian is

$$\begin{aligned} H_{2s} \;=\; & K_{Mn\text{-}Mn} S_1 \cdot S_2 + K_{Gd\text{-}Gd} J_1 \cdot J_2 \\ & + K_{Gd\text{-}Mn}(S_1 \cdot J_1 + S_2 \cdot J_2) \\ & + g\mu_B \left[(z-1)\vec{B}_{eff,Mn} + \vec{B}\right] \cdot [S_1 + S_2] \\ & + g\mu_B \left[(z-1)\vec{B}_{eff,Gd} + \vec{B}\right] \cdot [J_1 + J_2]\,. \end{aligned}$$

When the effective field is found, correlations between the different ions can be computed in the 2-site (four ions) cluster.

REFERENCES

[1] Jin S., Tiefel T. H., McCormack M., Fastnacht R. A., Ramesh R. and Chen L. H., *Science*, **264** (1994) 413.

[2] Ibarra M. R., Algarabel P. A., Marquina C., Blasco J. and García J., *Phys. Rev. Lett.*, **75** (1995) 3541.

[3] Kimura T., Tomioka Y., Asamitsu A. and Tokura Y., *Phys. Rev. Lett.*, **81** (1998) 5920.

[4] Hwang H. Y., Cheong S-W., Radaelli P. G., Marezio M. and Batlogg B., *Phys. Rev. Lett.*, **75** (1995) 914.

[5] Snyder G. Y., Booth C. H., Bridges F., Hiskes R., DiCarolis S., Beasley M. R. and Geballe T. H., *Phys. Rev. B*, **55** (1997) 6453.

[6] Hueso L. E., Rivas J., Sande P., Fondado A., Rivadulla F. and López-Quintella M. A., *J. Magn. & Magn. Mater.*, **238** (2002) 293.

[7] Peña O., Bahout M., Ghanimi K., Duran P., Gutierrez D. and Moure C., *J. Mater. Chem.*, **12** (2002) 2480.

[8] Żukrowski J., Waśniowska M., Tarnawski Z., Przewoźnik J., Chmist J., Kozlowski A. and Krop K., *Acta Phys. Pol. B*, **34** (2003) 1533.

[9] Haberkorn N., Larrégola S., Franco D. and Nieva G., *J. Magn. & Magn. Mater.*, **321** (2009) 1133.
[10] Correa V. F., Sänger N., Jorge G., Nieva G. and Haberkorn N., *J. Phys.: Conf. Ser.*, **167** (2009) 012010.
[11] Schmiedeshoff G. M., Lounsbury A. W., Luna D. J., Tracy S. J., Schramm A. J., Tozer S. W., Correa V. F., Hannahs S. T., Murphy T. P., Palm E. C., Lacerda A. H., Bud'ko S. L., Canfield P. C., Smith J. L., Lashley J. C. and Cooley J. C., *Rev. Sci. Instrum.*, **77** (2006) 123907.
[12] Van Kranendonk J. and Kasteleijn W., *Physica*, **22** (1956) 317.
[13] Smart J. S., *Effective Field Theories of Magnetism* (W. B. Saunders Company) 1966.
[14] Tudor Davies J., *Proc. Phys. Soc.*, **79** (1962) 821.
[15] Doerr M., Rotter M. and Lindbaum A., *Adv. Phys.*, **54** (2005) 1.
[16] Zapf V. S., Correa V. F., Sengupta P., Batista C. D., Tsukamoto M., Kawashima N., Egan P., Pantea C., Migliori A., Betts J. B., Jaime M. and Paduan-Filho A., *Phys. Rev. B*, **77** (2008) 020404(R).
[17] Srivastava A. and Gaur N. K., *J. Phys.: Conf. Ser.*, **215** (2010) 012140.
[18] Peña O., Bahout M., Gutierrez D., Duran P. and Moure C., *Solid State Sci.*, **5** (2003) 1217.
[19] Peña O., Bahout M., Ma Y., Gutierrez D., Duran P. and Moure C., *Physica C*, **408-410** (2004) 641.
[20] See, for instance, De Teresa J. M., Ibarra M. R., Algarabel P. A., Ritter C., Marquina C., Blasco J., García J., del Moral A. and Arnold Z., *Nature*, **386** (1997) 256.